JACS Au
AN OPEN ACCESS JOURNAL OF THE AMERICAN CHEMICAL SOCIETY

pubs.acs.org/jacsau
Letter

Organocatalytic Kinetic Resolution of Ferroceno[*c*]isoquinolines through Asymmetric Transfer Hydrogenation

Yan-Jiang Yu, Zheng Liu, Yi-Qian Yang, Mu-Wang Chen,* Rong-Zhen Liao, and Yong-Gui Zhou*

Cite This: *JACS Au* 2025, 5, 3765−3774
Read Online

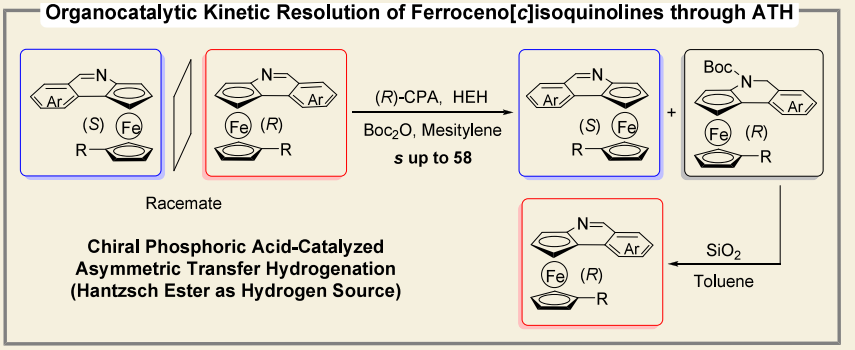

ABSTRACT: An efficient kinetic resolution of ferroceno[*c*]isoquinolines was realized through chiral phosphoric acid-catalyzed asymmetric transfer hydrogenation, affording the planar-chiral ferroceno[*c*]isoquinolines and planar-chiral *tert*-butyl ferroceno[*c*]-isoquinoline-4(5*H*)-carboxylates with a selectivity factor of up to 58. The *N*-Boc group could be easily removed from the reductive product. Moreover, the recovered materials could be transformed into various planar-chiral ferrocene-based bidentate ligands, which were successfully applied in several asymmetric catalytic reactions with excellent yields and enantioselectivities.

KEYWORDS: *Planar-chiral ferrocenes, Kinetic resolution, CPA catalysts, Asymmetric transfer hydrogenation*

Ferrocene was discovered and confirmed in the early 1950s.[1,2] Owing to its characteristic structural and electronic properties, the ferrocene derivatives have been extensively utilized in organic synthesis, pharmaceuticals, and material science (Figure 1).[3−6] It is of great importance to develop effective methods for the preparation of ferrocenes, especially for chiral ferrocene compounds, which play an important role not only in academic study but also in industrial applications. The most extensive and significant application of the planar-chiral ferrocenes lies in its role as a catalyst and ligand in asymmetric catalysis.[7,8] Regarded as one of the most successful instances of applications in industrialization,[9,10] (R,S_p)-xyliphos is a crucial ligand in iridium-catalyzed asymmetric hydrogenation for the synthesis of the chiral pesticide (*S*)-metolachlor.[11]

Construction of the planar-chiral ferrocenes has always attracted the continuous enthusiasm of chemists.[12−14] The classic methods for the synthesis of planar-chiral ferrocenes include: 1) diastereoselective directed *ortho*-metalation (DoM) with the central chiral auxiliary (Scheme 1A right)[15−17] and enantioselective DoM with chiral bases (Scheme 1A left),[18,19] 2) kinetic resolution of racemates,[20] and 3) semipreparative high-performance liquid chromatography technique separation.[21,22] Even though stoichiometric amounts of chiral bases or organolithium agents are required, some of these synthetic

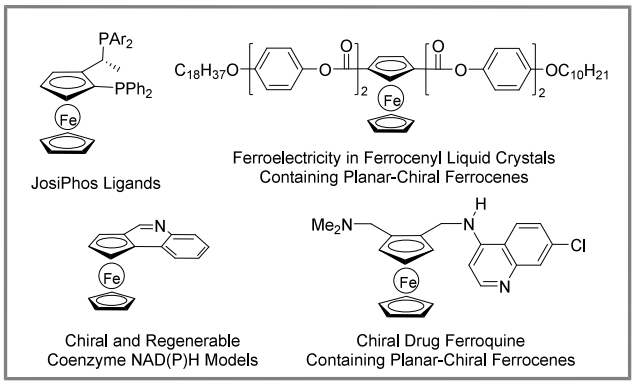

Figure 1. Selected planar-chiral ferrocene-based ligand, bioactive compound, catalyst, and liquid crystal material.

Received: June 5, 2025
Revised: July 30, 2025
Accepted: July 31, 2025
Published: August 5, 2025

https://doi.org/10.1021/jacsau.5c00698
JACS Au 2025, 5, 3765−3774

Scheme 1. Asymmetric Synthesis of Planar-Chiral Ferrocenes

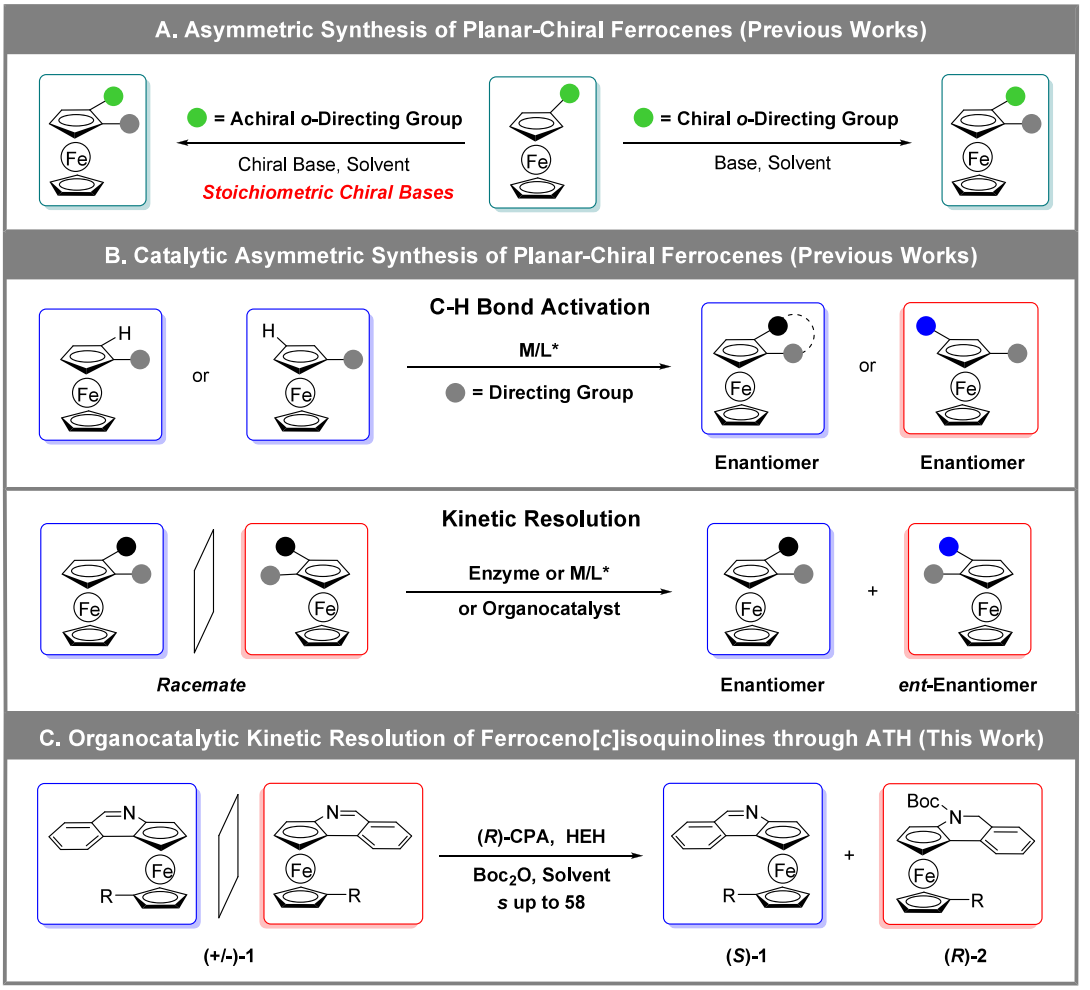

approaches are still employed for the synthesis of planar-chiral ferrocene-based ligands and catalysts.

Catalytic desymmetrization has been recognized as an effective strategy for constructing the planar-chiral ferrocenes; however, relevant reports are still rare.[23−25] Recently, the vigorous growth of transition metal-catalyzed asymmetric C−H functionalization has been witnessed,[26−28] and this strategy has also made some progress in the construction of planar-chiral ferrocenes. Since 1997, Siegel and Schmal reported the pioneering work on the synthesis of planar chiral ferrocene through copper-catalyzed enantioselective carbene C−H insertion.[29] Subsequently, an elegant method for the synthesis of planar-chiral ferrocenes via palladium-catalyzed C−H activation was achieved by You and co-workers.[30] Over the course of nearly three decades of development, catalytic asymmetric synthesis of planar-chiral ferrocenes through Pd,[31,32] Rh,[33,34] Ir,[35,36] Pt,[37] Au,[38,39] Co,[40] Ni,[41] Cu,[42,43] etc.[44] transition metal-catalyzed C−H bond activation/functionalization has been widely reported, which has significantly enriched the development of this field (Scheme 1B, C−H bond activation).[45−47] However, in most cases, this strategy often requires installation and removal of the directing group, which impedes further practical application. Consequently, there is an urgent need to develop practical methodologies for the catalytic asymmetric synthesis of planar-chiral ferrocene derivatives.

As is well-known, catalytic kinetic resolution of racemates is one of the most classical and effective approaches for the synthesis of optically active molecules, which enables the convenient construction of central,[48−51] axial,[52] planar,[53,54] and helical chirality.[55] Catalytic kinetic resolution for the synthesis of planar-chiral ferrocenes is also a promising and reliable approach. In 1989, the Yamazaki group reported the first enzymatic kinetic resolution of a planar-chiral ferrocene.[56] Since then, many enzyme-catalyzed systems have been applied for the kinetic resolution of planar-chiral ferrocenes.[20,57,58] Compared with enzymatic kinetic resolution, nonenzymatic kinetic resolution is achieved through the chiral catalysts, including metal catalysts and organocatalysts. The first example of metal-catalyzed kinetic resolution to synthesize planar chiral ferrocenes was reported by the Moyano group in 2006.[59] At the same time, the Ogasawara group also initiated the development of kinetic resolution through transition metal-catalyzed asymmetric ring-closing metathesis for the construction of planar-chiral metallocene compounds, including planar-chiral ferrocenes.[60,61] In 2009, the Rios and Moyano group reported the organocatalytic kinetic resolution of a planar-chiral ferrocene.[62] Up to now, certain progress has been achieved in the synthesis of planar-chiral ferrocenes via catalytic kinetic resolution (Scheme 1B, kinetic resolution).[63−67] Hence, it is of great significance to enrich and

https://doi.org/10.1021/jacsau.5c00698
JACS Au 2025, 5, 3765−3774

Table 1. Evaluation of Reaction Parameters[a]

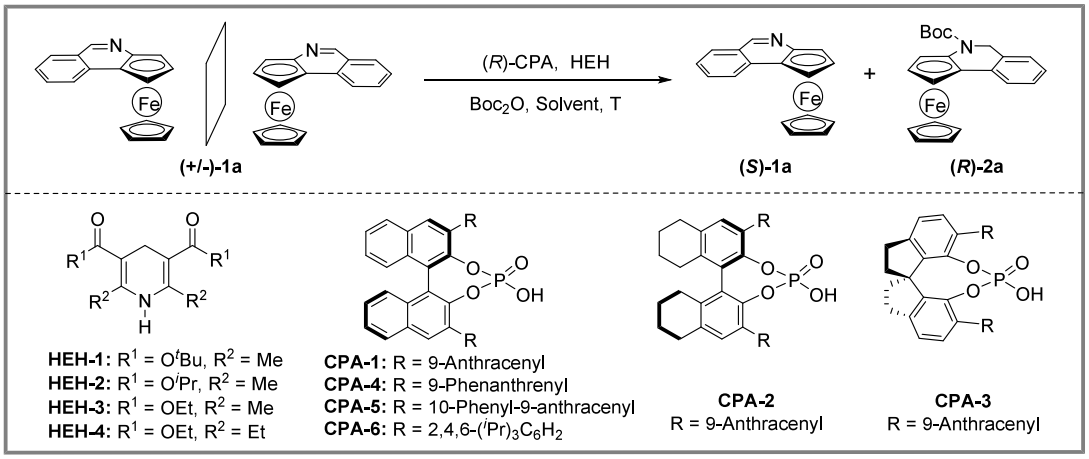

				1a		2a		
entry	solvent	HEH	CPA	yield (%)[b]	ee (%)[c]	yield (%)[b]	ee (%)[c]	s[d]
1	toluene	HEH-1	CPA-1	42	85.7	52	78.0	22.0
2	*m*-xylene	HEH-1	CPA-1	40	89.3	53	75.5	21.2
3	mesitylene	HEH-1	CPA-1	42	96.2	55	77.6	30.8
4	$PhCF_3$	HEH-1	CPA-1	42	64.1	52	58.5	7.2
5	CH_2Cl_2	HEH-1	CPA-1	44	44.0	53	36.3	3.2
6	THF	HEH-1	CPA-1	54	31.9	45	38.8	3.0
7	mesitylene	HEH-2	CPA-1	40	96.6	58	67.1	19.8
8	mesitylene	HEH-3	CPA-1	35	99.6	65	54.7	19.0
9	mesitylene	HEH-4	CPA-1	35	99.8	65	54.5	20.8
10	mesitylene	HEH-1	CPA-2	39	97.9	60	66.1	21.1
11	mesitylene	HEH-1	CPA-3	39	97.0	59	64.6	18.5
12	mesitylene	HEH-1	CPA-4	52	51.9	44	64.5	7.7
13	mesitylene	HEH-1	CPA-5	43	97.8	55	76.7	33.1
14	mesitylene	HEH-1	CPA-6	56	42.1	40	57.3	5.5
15[e]	mesitylene	HEH-1	CPA-5	43	98.1	56	74.1	30.1
16[f]	mesitylene	HEH-1	CPA-5	44	93.8	52	87.1	50.7
17[g]	**mesitylene**	**HEH-1**	**CPA-5**	**46**	**92.2**	**50**	**88.3**	**53.0**
18[h]	mesitylene	HEH-1	CPA-5	44	95.0	52	86.0	49.0
19[i]	mesitylene	HEH-1	CPA-5	45[j]	93.6	48[j]	87.8	53.4

[a]Reaction conditions: (±)-**1a** (0.2 mmol), CPA (5.0 mol %), HEH (1.0 equiv), Boc_2O (1.0 equiv) Solvent (4.0 mL), 50 °C, 11 h. [b]Yield was measured by analysis of ^1H NMR spectra, using mesitylene as the internal standard. [c]Determined by chiral HPLC. [d]Calculated conversion and selectivity factors: $C = ee_{1a}/(ee_{1a} + ee_{2a})$, $s = \ln[(1 - C)(1 - ee_{1a})]/\ln[(1 - C)(1 + ee_{1a})]$. [e]40 °C. [f]HEH (0.7 equiv). [g]Mesiytlene (5.0 mL). [h](*R*)-CPA-**5** (2.5 mol %). [i]The reaction conducted at 0.40 mmol scale. [j]Isolated yield.

develop novel and efficient methods for the synthesis of planar chiral ferrocenes via kinetic resolution.

Asymmetric (transfer) hydrogenation of heteroaromatics has emerged as one of the most streamlined and atomically efficient methodologies for the synthesis of chiral heterocyclic compounds.[68−70] Our group has always been committed to the homogeneous asymmetric hydrogenation of heteroaromatics and has accomplished the concise and efficient synthesis of multiple types of chiral heterocyclic compounds.[71,72] In 2016, we achieved kinetic resolution of axially chiral biaryl compounds with excellent selectivity factor (s up to 209) via asymmetric transfer hydrogenation.[73] Based on the diverse structures and functions of planar-chiral ferrocenes, various planar chiral ferrocene-fused heterocyclic molecules have been developed as highly efficient catalysts for asymmetric synthesis.[74] We envisaged synthesis of the ferrocene-fused heterocyclic molecules through asymmetric transfer hydrogenation of readily available racemic planar-chiral ferroceno[*c*]isoquinolines. The key is to look for an effective method to hydrogenate aromatic compounds while also being able to distinguish the chiral planarity of ferrocene-fused heterocyclics. Herein, we report a chiral phosphoric acid (CPA)-catalyzed asymmetric transfer hydrogenation of heteroaromatics for kinetic resolution of the readily available ferroceno[*c*]-isoquinolines, affording both configurationally planar-chiral ferroceno[*c*]isoquinolines, with a kinetic resolution selectivity factor as high as 58.1 (Scheme 1C).

Initially, the kinetic resolution of ferroceno[*c*]isoquinoline (±)-**1a** was investigated *via* asymmetric transfer hydrogenation using CPA as the catalyst and Hantzsch ester (HEH) as the hydrogen source. In the presence of 5 mol % of (*R*)-CPA-**1** and 1.0 equiv of HEH-**1** in toluene at 50 °C, the chiral hydrogenation product ferroceno[*c*]dihydroisoquinolines **2a′** and the recovered substrate **1a** could be observed. However, **2a′** would rapidly return to substrate **1a** due to the driving force for dehydroaromatization, which was a challenge to overcome. Previously, our group reported that ferrocene-based regenerable and chiral NAD(P)H models FENAM contain

https://doi.org/10.1021/jacsau.5c00698
JACS Au 2025, 5, 3765−3774

Scheme 2. Substrate Scope[a]

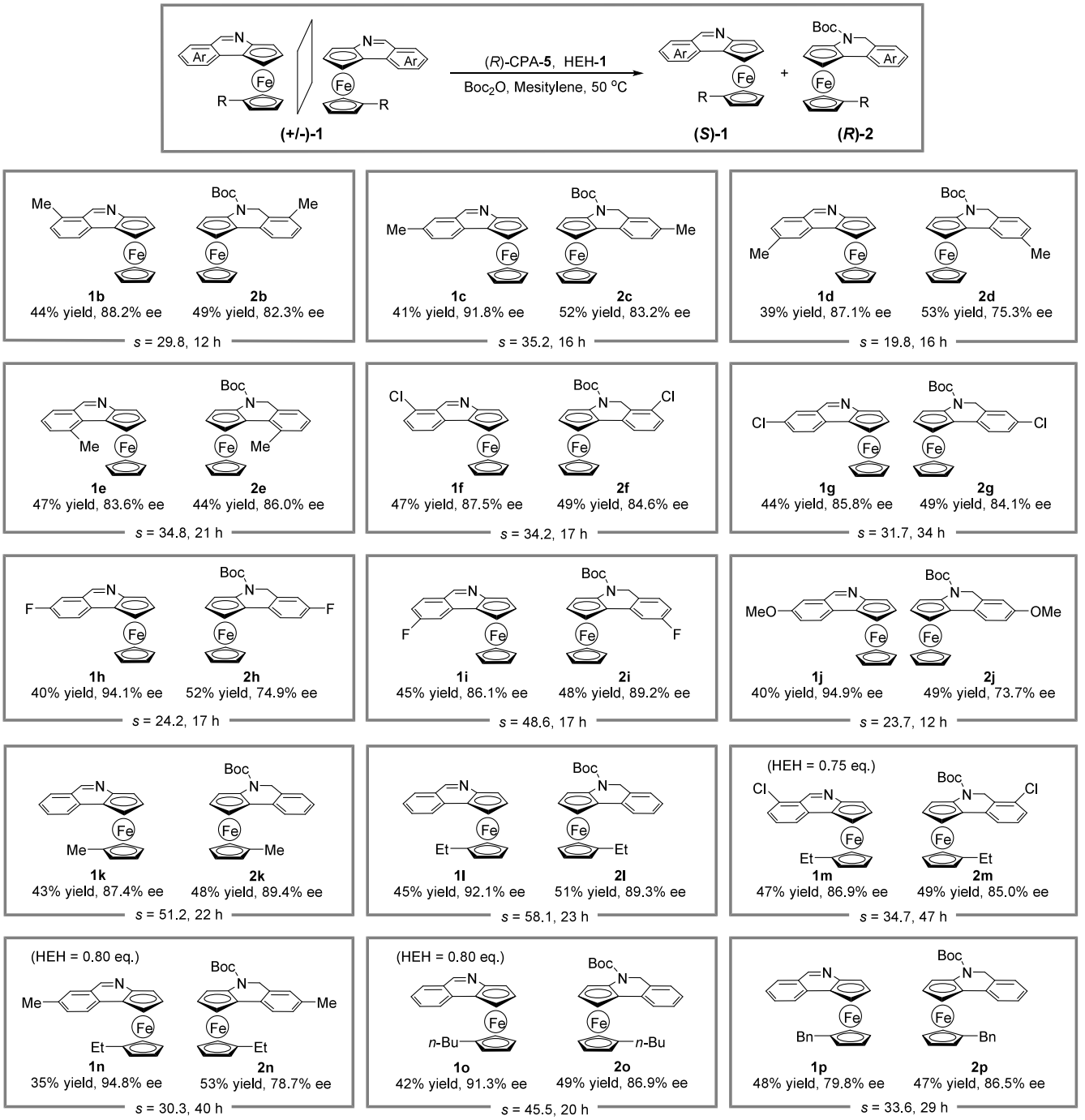

[a]Reaction conditions: Ferroceno[*c*]isoquinolines (±)-**1** (0.4 mmol), catalyst (*R*)-CPA-**5** (5.0 mol %), HEH-**1** (0.7 equiv), Boc_2O (1.0 equiv), mesitylene (10.0 mL), 50 °C. Isolated yields. The ee values were determined by chiral HPLC

structural units similar to dihydrophenanthridine, which have been successfully applied in asymmetric reduction and synthesis of the chiral heterocyclics.[75−79] Considering that the substrate ferroceno[*c*]isoquinolines have a similar structural moiety, we wondered whether we could *in situ* protect the product during hydrogenation by adding a protecting group so that it could be stably separated. At the same time, removing the protecting group could serve as a chiral NAD(P)H model. To our delight, the desired product **2a** was obtained by *in situ* protection of the NH of hydrogenation product ferroceno[*c*]-dihydroisoquinoline **2a′** with di-*t*-butyl dicarbonate in the system. The desired product **2a** and the recovered substrate **1a** were obtained with 78.0% ee (53% yield) and 85.7% ee (42% yield), respectively (Table 1, entry 1, *s* = 22.0). After solving the separable issue, we officially began the exploration of the optimal reaction parameters. Initially, the effect of different solvents, such as *m*-xylene, mesitylene, benzotrifluoride ($PhCF_3$), dichloromethane (DCM), and tetrahydrofuran (THF) on the reactivity and selectivity factors was evaluated (entries 2−6). As a result, the selectivity factors of toluene, *m*-xylene, and mesitylene were all greater than 20.0. The kinetic resolution with DCM or THF exhibited poor selectivity factors

https://doi.org/10.1021/jacsau.5c00698
JACS Au 2025, 5, 3765−3774

Scheme 3. Scale-up Synthesis, Derivatizations, and Applications

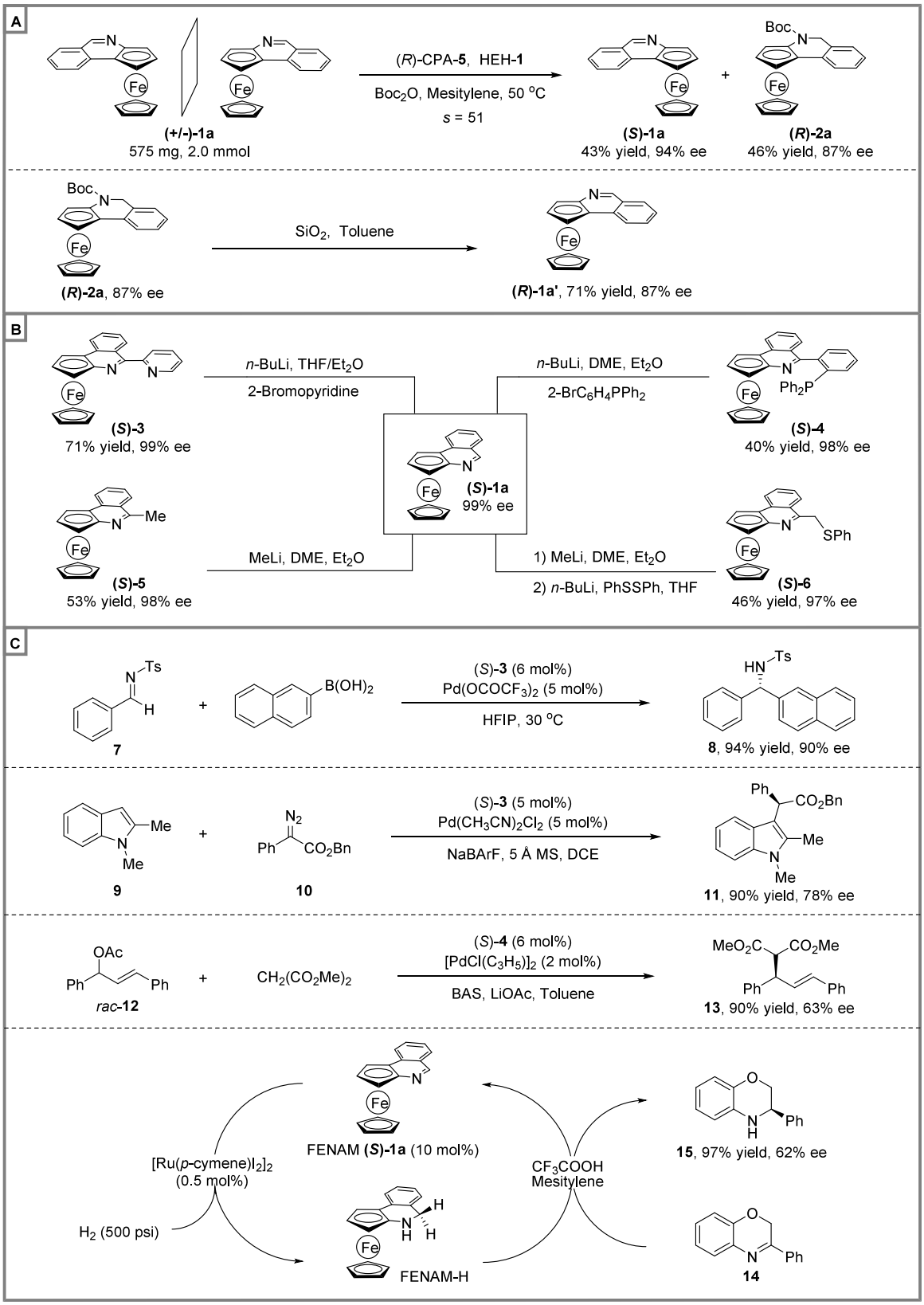

(entries 5−6). A survey of solvents indicated that mesitylene was the best choice, which displayed the highest selectivity factor (entry 3, s = 30.8). As we know, Hantzsch esters (HEH) usually played a crucial role in asymmetric transfer hydrogenation, and the effect of various Hantzsch esters (HEH) on the selectivity factors was investigated (entries 3, 7−9). It was found that the steric hindrance of substituents on HEH has a great influence, and introducing a large steric effect group (*t*-

https://doi.org/10.1021/jacsau.5c00698
JACS Au 2025, 5, 3765−3774

butyl) on R^1 would provide the best kinetic resolution selectivity (entry 3, s = 30.8). However, the influence of R^2 was marginal on kinetic resolution selectivity. Next, a series of commercially available CPA catalysts were also examined (entries 10−14), showing that the BINOL-derived catalysts with a bulky 10-phenyl-9-anthracenyl group at 3,3′-positions afforded the best kinetic resolution selectivity (entry 13, s = 33.1, ee_{1a} = 97.8%, ee_{2a} = 76.7%). When the temperature was decreased from 50 to 40 °C, the selectivity factor decreased slightly to 30.1 (entries 13 and 15, s = 33.1 and 30.1). To our delight, the selectivity factors of the reaction significantly increased to 50.7, when the amounts of HEH-**1** were reduced from 1.0 to 0.7 equiv (entries 13 and 16, s = 33.1 and 50.7). In addition, when the amount of mesitylene was increased from 4 to 5 mL, the s value slightly increased to 53.0 (entries 16 and 17, s = 50.7 and 53.0). Subsequently, decreasing the catalyst loading by half to 2.5 mol %, the s value slightly dropped to 49.0 (entries 17 and 18, s = 53.0 and 49.0). However, in order to ensure the robustness of the kinetic resolution, we still employed catalyst loading to 5.0 mol %. When kinetic resolution of the model substrate ferroceno[c]isoquinoline (±)-**1a** occurred through the CPA-catalyzed asymmetric transfer hydrogenation at 0.40 mmol under the optimal reaction conditions, the desired product **2a** and the recovered substrate **1a** were obtained with 93.6% ee (45% yield) and 87.8% ee (48% yield), respectively, and the selectivity factor was 53.4 (entry 19). Therefore, the optimal reaction parameters were established as mesitylene/HEH-**1**/(*R*)-CPA-**5**/50 °C.

With the optimized conditions in hand, we began to explore the substrate scope of kinetic resolution of ferroceno[c]-isoquinolines **1** through asymmetric transfer hydrogenation, and the results are summarized in Scheme 2. The approach was capable of attaining the kinetic resolution for different kinds of ferroceno[c]isoquinolines smoothly, and the s values were all satisfactory (19.8−58.1). First, the reactions could be carried out with good kinetic resolution selectivity (19.8−35.2), when a methyl group was attached to a different position on the benzene ring of the isoquinoline unit (**1b**−**1e**). Subsequently, we examined the electronic effect of substituents on the benzene ring. The substrates containing the electron-withdrawing group, the halogen substituent, were well tolerated and afforded the corresponding hydrogenation products (**1f**, **1g**, **1h**, **1i**, s = 34.2, 31.7, 24.2, 48.6). Among them, the substrate bearing a fluorine atom (**1i**) obtained a selectivity factor of nearly 50. Besides, when a methoxy substituent was introduced to the benzene ring of ferroceno[c]isoquinolines, the selectivity factor was 23.7 (**1j**). The results suggested that selectivity factors were insensitive to the electronic effect. Moreover, ferroceno[c]isoquinolines with various substituents on the other Cp ring, including methyl (**1k**), ethyl (**1l**), *n*-butyl (**1o**), and benzyl (**1p**), were investigated under the optimized conditions with satisfactory selectivity factors (33.6−58.1). It is important to highlight that the ethyl-substituted substrate obtained an optimal selectivity factor in this work (**1l**, s = 58.1). Consequently, based on the substrate **1l**, we further investigated two ferroceno[c]isoquinoline substrates bearing chlorine (**1m**) and methyl (**1n**), respectively, and the high selectivity factors were observed (**1m**, **1n**, s = 34.7, 30.3). The absolute configuration of the recovered substrate **1g** was assigned to be (*S*) by one-step transformation to a known compound and comparison of its specific optical rotation with the value in the literature,[80] and the configuration of the desired product was (*R*) by analogue. The details are described in the Supporting Information.

In order to demonstrate the synthetic utility of this methodology, a 2.0 mmol scale was conducted using racemic ferroceno[c]isoquinolines **1a** under the optimal reaction conditions. The desired product **2a** was isolated in 46% yield with 87% ee, and the recovered substrate **1a** was obtained in 43% yield with 94% ee without a loss of reactivity and enantioselectivity (s = 51). Notably, the Boc protective group could be readily removed in the presence of silica gel in refluxing toluene without a loss of enantioselectivity (Scheme 3A). In this way, both configurational planar-chiral ferroceno-[c]isoquinolines could be obtained. This demonstrated that our methodology has potential application in the facile synthesis of chiral NAD(P)H models. Furthermore, considering that planar chiral ferrocenyl ligands are widely employed in asymmetric catalytic reactions, various types of planar-chiral ferrocene-based bidentate ligands could be easily prepared from recovered substrate (*S*)-**1a** (99% ee). As shown in Scheme 3, starting from (*S*)-**1a**, the planar-chiral *N*,*N*-ligand (*S*)-**3** could be synthesized in 71% yield and 99% ee in the presence of 2-lithiopyridine (*in situ* prepared). In the same way, the planar-chiral *N*,*P*-ligand (*S*)-**4** could be conveniently synthesized from the recovered substrate (*S*)-**1a** (99% ee) with *o*-lithiated diphenylphenylphosphine (*in situ* prepared). The (*S*)-**6**, which may serve as a potential planar-chiral *N*,*S*-ligand for some asymmetric transformations, was also synthesized from (*S*)-**5** prepared from (*S*)-**1a** (99% ee) (Scheme 3B). Fortunately, the enantioselectivities of all of the ligands obtained above were maintained.

After synthesizing a series of chiral ligands, we applied them to asymmetric catalytic reactions. To our delight, the planar-chiral *N*,*N*-bidentate ligand (*S*)-**3** could be applied in palladium-catalyzed asymmetric arylation of *N*-tosylimine **7** with 2-naphthaleneboronic acid, and the corresponding product **8** was obtained in 94% yield and 90% ee. Besides, enantioselective palladium-catalyzed C−H functionalization of indole **9** with benzyl 2-diazo-2-phenylacetate **10** could proceed smoothly, affording the corresponding product in 90% yield and 78% ee. When the planar-chiral *N*,*P*-ligand (*S*)-**4** was examined in palladium-catalyzed asymmetric allylic substitution, alkylation product **13** was obtained with an excellent yield and moderate 63% enantioselectivity. In addition, planar-chiral ferroceno[c]isoquinoline have a structural moiety similar to that of the regenerable coenzyme NAD(P)H model FENAM, so we applied it to the biomimetic asymmetric reduction reaction of benzoxazinone. The desirable reductive product dihydrobenzoxazinone **15** could be obtained with 97% yield and 62% ee using trifluoroacetic acid as the transfer catalyst and the homogeneous ruthenium complex as the regeneration catalyst (Scheme 3C).

To further investigate whether the enantioselectivity depends on the hydrogenation step, the *N*-Boc protection step, or both, we carried out two control experiments (Scheme 4). The first control experiment involved the asymmetric transfer hydrogenation of ferrocene[c]isoquinoline (±)-**1a**, conducted in the absence of *N*-Boc protection of the reduction product. The hydrogenation product **2a′** and the recovered substrate **1a** were obtained with 93.1% ee and 63.4% ee, respectively, and the s value was 53.8 (Scheme 4A), which was similar to the s value (53.4) under standard conditions. The second control experiment was the *N*-Boc protection of the hydrogenation product (±)-**2a′** without HEH-1 under stand-

https://doi.org/10.1021/jacsau.5c00698
JACS Au 2025, 5, 3765−3774

Scheme 4. Control Experiments

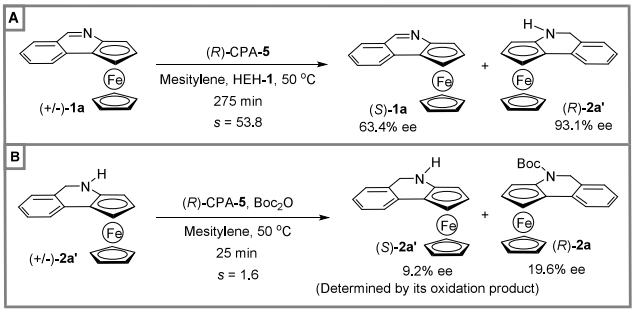

ard conditions. The *N*-Boc protection product **2a** and the recovered ferroceno[*c*]dihydroisoquinoline **2a′** (ee value was determined by its oxidation product) were obtained with 19.6% ee and 9.2% ee, respectively, and the *s* value was 1.6 (Scheme 4 B). The results of the control experiments implied that the asymmetric transfer hydrogenation step plays the most significant role in enantioselectivity control.

To further provide strong evidence for the origin of the enantioselectivity, we carried out DFT calculations, the details of which are described in the Supporting Information. With (*R*)-CPA-**5** as the catalyst, the transfer hydrogenation between HEH-**1** and **1a** from React can take place via a concerted transition state **TS1** (Figure 2), similar to the transfer hydrogenation between Hantzsch ester and imine.[81] The barrier for (*R*)-**TS1** is 14.8 kcal/mol, while it is 7.8 kcal/mol higher for (*S*)-**TS1**. The first step to form (*R*)-**Int1** is exergonic by 1.7 kcal/mol. The local environment for the reaction center in React was analyzed by using the steric contour map (Figure S2) proposed by the Cavallo group. The whole map is divided into four parts, namely, northeast (NE), southeast (SE), southwest (SW), and northwest (NW). The Hantzsch ester is located in zones NE and NW; thus, zones SW and SE accommodate the ferroceno[*c*]isoquinoline substrate, and zone SW prefers to accommodate the ferroceno moieties during the transfer hydrogenation. Interestingly, transfer hydrogenation could also take place between (*R*)-**2a′** and (*S*)-**1a** through **TS2**, which has a barrier of 14.5 kcal/mol relative to (*R*)-**Int2**. These results demonstrated that even though direct transfer hydrogenation between HEH-**1** and (*S*)-**1a** is very unfavorable (*S*)-**2a′** could be produced using (*R*)-**2a′** as the H_2 surrogate and phosphoric acid as the catalyst.

It should be noted that the energy difference between **TS2** and (*R*)-**TS1** for the second transfer hydrogenation cycle is 2.8 kcal/mol (Figure S4), which explains the high stereoselectivity shown in Scheme 4A.

For the following *N*-Boc protection, the calculations showed that **2a′** could react with di-*t*-butyl dicarbonate directly via **TS3′** with a barrier of 19.4 kcal/mol (Figure S5). With the assistance of phosphoric acid, the barrier decreases by several

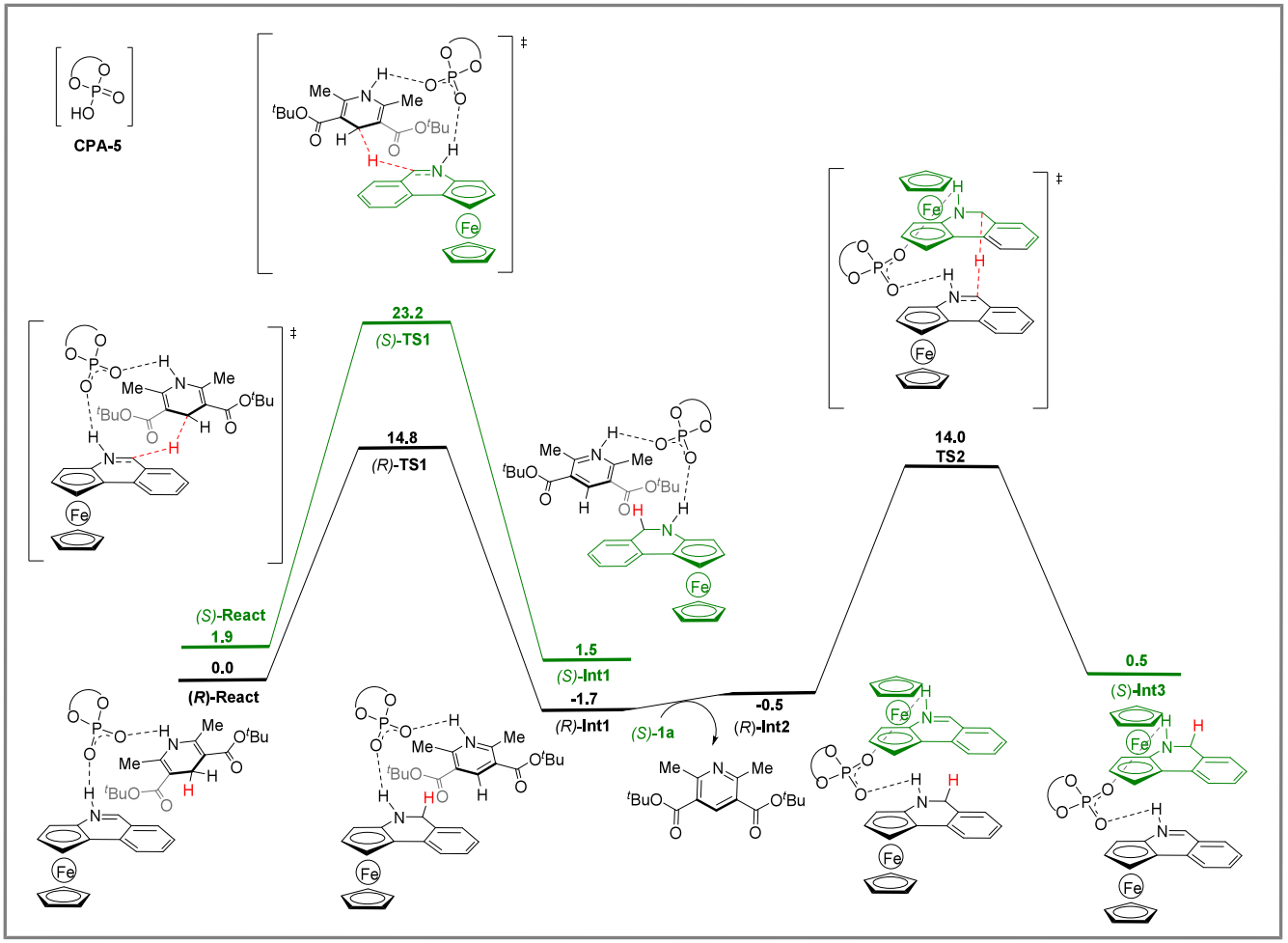

Figure 2. Gibbs energy profile (in kcal/mol) for the transfer hydrogenation of substrate (*R*/*S*)-**1a** catalyzed by CPA-**5**.

https://doi.org/10.1021/jacsau.5c00698
JACS Au 2025, 5, 3765−3774

kilocalories per mole (Figure S6). However, under catalytic conditions, phosphoric acid is mainly involved in the transfer hydrogenation step, as the total barrier for the uncatalyzed *N*-Boc protection reaction (19.4 kcal/mol) is even lower than that for the phosphoric acid catalyzed reaction ((*R*)-**TS3**, 24.2 kcal/mol relative to (*R*)-**Int1**, Figure S7). The completion of the uncatalyzed and catalyzed *N*-Boc protection reactions rationalizes the low stereoselectivity observed in Scheme 4B.

In summary, we have developed a new approach for the synthesis of planar-chiral ferroceno[*c*]isoquinolines via kinetic resolution by chiral phosphoric acid-catalyzed asymmetric transfer hydrogenation with a kinetic resolution selectivity factor as high as 58. To the best of our knowledge, this methodology provides the first example of accessing planar-chiral ferrocene-fused *N*-heteroaromatics via asymmetric transfer hydrogenation. Moreover, the planar-chiral ferroceno-[*c*]isoquinolines synthesized through our kinetic resolution platform are smoothly transformed into various novel ligands and serve as chiral and regenerable coenzyme NAD(P)H models in biomimetic asymmetric reduction. Our future studies focus on this methodology toward kinetic resolution of other planar chiral molecules and applications of the original planar-chiral ferrocene ligands.

■ ASSOCIATED CONTENT

Data Availability Statement

The data underlying this study are available in the published article and its Supporting Information.

Supporting Information

The Supporting Information is available free of charge at https://pubs.acs.org/doi/10.1021/jacsau.5c00698.

Experimental procedures, characterization data, and NMR spectra (PDF)

■ AUTHOR INFORMATION

Corresponding Authors

Mu-Wang Chen − *State Key Laboratory of Catalysis, Dalian Institute of Chemical Physics, Chinese Academy of Sciences, Dalian 116023, China;* orcid.org/0000-0001-6493-1363; Email: chemmuwang@dicp.ac.cn

Yong-Gui Zhou − *State Key Laboratory of Catalysis, Dalian Institute of Chemical Physics, Chinese Academy of Sciences, Dalian 116023, China; State Key Laboratory of Organometallic Chemistry, Shanghai Institute of Organic Chemistry, Chinese Academy of Sciences, Shanghai 200032, China;* orcid.org/0000-0002-3321-5521; Email: ygzhou@dicp.ac.cn

Authors

Yan-Jiang Yu − *School of Chemistry, Dalian University of Technology, Dalian 116024, China*

Zheng Liu − *State Key Laboratory of Catalysis, Dalian Institute of Chemical Physics, Chinese Academy of Sciences, Dalian 116023, China*

Yi-Qian Yang − *School of Chemistry and Chemical Engineering, Huazhong University of Science and Technology, Wuhan 430074, China*

Rong-Zhen Liao − *School of Chemistry and Chemical Engineering, Huazhong University of Science and Technology, Wuhan 430074, China;* orcid.org/0000-0002-8989-6928

Complete contact information is available at: https://pubs.acs.org/10.1021/jacsau.5c00698

Notes

The authors declare no competing financial interest.

■ ACKNOWLEDGMENTS

Financial support from National Natural Science Foundation of China (22371276), Dalian Institute of Chemical Physics (DICP I202404), United Foundation for DICP and the Second Hospital of Dalian Medical University (DMU2&DICP UN202409), and the Energy Revolution S&T Program of Yulin Innovation Institute of Clean Energy (E412020705) is acknowledged.

■ REFERENCES

(1) Kealy, T. J.; Pauson, P. L. A New Type of Organo-Iron Compound. *Nature* **1951**, *168*, 1039−1040.

(2) Wilkinson, G.; Rosenblum, M.; Whiting, M. C.; Woodward, R. B. The Structure of Iron Bis-Cyclopentadienyl. *J. Am. Chem. Soc.* **1952**, *74*, 2125−2126.

(3) Hayashi, T., Togni, A., Eds. *Ferrocenes: Homogeneous Catalysis, Organic Synthesis, Materials Science*; VCH: Weinheim, Germany, 1995.

(4) Xiao, X.; Xu, K.; Gao, Z.-H.; Zhu, Z.-H.; Ye, C.; Zhao, B.; Luo, S.; Ye, S.; Zhou, Y.-G.; Xu, S.; Zhu, S.-F.; Bao, H.; Sun, W.; Wang, X.; Ding, K. Biomimetic Asymmetric Catalysis. *Sci. Chin. Chem.* **2023**, *66*, 1553−1633.

(5) Patra, M.; Gasser, G. The Medicinal Chemistry of Ferrocene and Its Derivatives. *Nat. Rev. Chem.* **2017**, *1*, 66−77.

(6) Chuard, T.; Cowling, S. J.; Fernandez-Ciurleo, M.; Jauslin, I.; Goodby, J. W.; Deschenaux, R. Planar Chirality: A Fascinating Symmetry Breaking Which Leads to Ferroelectricity in Ferrocenyl Liquid Crystals. *Chem. Commun.* **2000**, *36*, 2109−2110.

(7) Dai, L.-X.; Hou, X.-L., Eds. *Chiral Ferrocenes in Asymmetric Catalysis Synthesis and Applications*; VCH: Weinheim, Germany, 2009.

(8) Cunningham, L.; Benson, A.; Guiry, P. J. Recent Developments in the Synthesis and Applications of Chiral Ferrocene Ligands and Organocatalysts in Asymmetric Catalysis. *Org. Biomol. Chem.* **2020**, *18*, 9329−9370.

(9) Blaser, H.-U.; Brieden, W.; Pugin, B.; Spindler, F.; Studer, M.; Togni, A. Solvias Josiphos Ligands: From Discovery to Technical Applications. *Top. Catal.* **2002**, *19*, 3−16.

(10) Blaser, H.-U.; Pugin, B.; Spindler, F. Progress in Enantioselective Catalysis Assessed from an Industrial Point of View. *J. Mol. Catal. A: Chem.* **2005**, *231*, 1−20.

(11) Blaser, H.-U. The Chiral Switch of (*S*)-Metolachlor: A Personal Account of An Industrial Odyssey in Asymmetric Catalysis. *Adv. Synth. Catal.* **2002**, *344*, 17−31.

(12) Richards, C. J.; Locke, A. J. Recent Advances in the Generation of Non-racemic Ferrocene Derivatives and Their Application to Asymmetric Synthesis. *Tetrahedron: Asymmetry* **1998**, *9*, 2377−2407.

(13) Atkinson, R. C. J.; Gibson, V. C.; Long, N. J. The Syntheses and Catalytic Applications of Unsymmetrical Ferroceneligands. *Chem. Soc. Rev.* **2004**, *33*, 313−328.

(14) Schaarschmidt, D.; Lang, H. Selective Syntheses of Planar-Chiral Ferrocenes. *Organometallics* **2013**, *32*, 5668−5704.

(15) Marquarding, D.; Klusacek, H.; Gokel, G.; Hoffmann, P.; Ugi, I. Stereoselective Syntheses. VI. Correlation of Central and Planar Chirality in Ferrocene Derivatives. *J. Am. Chem. Soc.* **1970**, *92*, 5389−5393.

(16) Rebière, F.; Riant, O.; Ricard, L.; Kagan, H. B. Asymmetric Synthesis and Highly Diastereoselective *ortho*-Lithiation of Ferrocenyl Sulfoxides. Application to the Synthesis of Ferrocenyl Derivatives with Planar Chirality. *Angew. Chem., Int. Ed.* **1993**, *32*, 568−570.

(17) Riant, O.; Samuel, O.; Flessner, T.; Taudien, S.; Kagan, H. B. An Efficient Asymmetric Synthesis of 2-Substituted Ferrocenecarboxaldehydes. *J. Org. Chem.* **1997**, *62*, 6733−6745.

(18) Aratani, T.; Gonda, T.; Nozaki, H. Asymmetric Lithiation of Ferrocenes. *Tetrahedron* **1970**, *26*, 5453−5464.
(19) Tsukazaki, M.; Tinkl, M.; Roglans, A.; Chapell, B. J.; Taylor, N. J.; Snieckus, V. Direct and Highly Enantioselective Synthesis of Ferrocenes with Planar Chirality by (−)-Sparteine-Mediated Lithiation. *J. Am. Chem. Soc.* **1996**, *118*, 685−686.
(20) Alba, A.-N. R.; Rios, R. Kinetic Resolution: A Powerful Tool for the Synthesis of Planar-Chiral Ferrocenes. *Molecules* **2009**, *14*, 4747−4757.
(21) Ruble, J. C.; Fu, G. C. Chiral π-Complexes of Heterocycles with Transition Metals: A Versatile New Family of Nucleophilic Catalysts. *J. Org. Chem.* **1996**, *61*, 7230−7231.
(22) Sechi, B.; Cossu, S.; Peluso, P. Enantioseparation of Organometallic Compounds and Metal Complexes by Liquid Chromatographic Techniques. A Review. *J. Chromatogr. Open* **2024**, *6*, 100147.
(23) Genet, C.; Canipa, S. J.; O'Brien, P.; Taylor, S. Catalytic Asymmetric Synthesis of Ferrocenes and P-Stereogenic Bisphosphines. *J. Am. Chem. Soc.* **2006**, *128*, 9336−9337.
(24) Lv, X.; Xu, J.; Sun, C.; Su, F.; Cai, Y.; Jin, Z.; Chi, Y. R. Access to Planar Chiral Ferrocenes *via* *N*-Heterocyclic Carbene-Catalyzed Enantioselective Desymmetrization Reactions. *ACS Catal.* **2022**, *12*, 2706−2713.
(25) Qi, H.; Hang, N.-N.; Ming, J. Synthesis of Planar Chiral Ferrocenes by Catalytic Desymmetrization Reactions. *ChemCatChem.* **2024**, *16*, No. e202400736.
(26) You, S.-L. *Asymmetric Functionalization of C-H Bonds*; Royal Society of Chemistry, 2015.
(27) Newton, C. G.; Wang, S.-G.; Oliveira, C. C.; Cramer, N. Catalytic Enantioselective Transformations Involving C-H Bond Cleavage by Transition-Metal Complexes. *Chem. Rev.* **2017**, *117*, 8908−8976.
(28) Shao, Q.; Wu, K.; Zhuang, Z.; Qian, S.; Yu, J.-Q. From $Pd(OAc)_2$ to Chiral Catalysts: The Discovery and Development of Bifunctional Mono-*N*-Protected Amino Acid Ligands for Diverse C-H Functionalization Reactions. *Acc. Chem. Res.* **2020**, *53*, 833−851.
(29) Siegel, S.; Schmalz, H.-G. Insertion of Carbenoids into Cp-H Bonds of Ferrocenes: An Enantioselective-Catalytic Entry to Planar-Chiral Ferrocenes. *Angew. Chem., Int. Ed.* **1997**, *36*, 2456−2458.
(30) Gao, D.-W.; Shi, Y.-C.; Gu, Q.; Zhao, Z.-L.; You, S.-L. Enantioselective Synthesis of Planar Chiral Ferrocenes *via* Palladium-Catalyzed Direct Coupling with Arylboronic Acids. *J. Am. Chem. Soc.* **2013**, *135*, 86−89.
(31) Liu, L.-T.; Zhang, A.-A.; Zhao, R.-J.; Li, F.; Meng, T.-J.; Ishida, N.; Murakami, M.; Zhao, W.-X. Asymmetric Synthesis of Planar Chiral Ferrocenes by Enantioselective Intramolecular C-H Arylation of *N*-(2-Haloaryl)-ferrocenecarboxamides. *Org. Lett.* **2014**, *16*, 5336−5338.
(32) Lv, X.; Wang, M.; Zhao, Y.; Shi, Z. P(III)-Directed Asymmetric C-H Arylation toward Planar Chiral Ferrocenes by Palladium Catalysis. *J. Am. Chem. Soc.* **2024**, *146*, 3483−3491.
(33) Liu, C.-X.; Zhao, F.; Gu, Q.; You, S.-L. Enantioselective Rh(I)-Catalyzed C-H Arylation of Ferroceneformaldehydes. *ACS Cent. Sci.* **2023**, *9*, 2036−2043.
(34) Thorat, R. A.; Parganiha, D.; Jain, S.; Choudhary, V.; Shakir, B.; Rohilla, K.; Jha, R. K.; Kumar, S. Temperature-Dependent Diastereodivergent [4 + 3] Annulation: Synthesis of Ferrocene-Fused Azepines *via* Rh(III) Catalysis. *Org. Lett.* **2025**, *27*, 552−558.
(35) Shibata, T.; Shizuno, T. Iridium-Catalyzed Enantioselective C-H Alkylation of Ferrocenes with Alkenes Using Chiral Diene Ligands. *Angew. Chem., Int. Ed.* **2014**, *53*, 5410−5413.
(36) Zou, X.; Li, Y.; Ke, Z.; Xu, S. Chiral Bidentate Boryl Ligand-Enabled Iridium-Catalyzed Enantioselective Dual C-H Borylation of Ferrocenes: Reaction Development and Mechanistic Insights. *ACS Catal.* **2022**, *12*, 1830−1840.
(37) Shibata, T.; Uno, N.; Sasaki, T.; Kanyiva, K. S. Pt-Catalyzed Enantioselective Cycloisomerization for the Synthesis of Planar-Chiral Ferrocene Derivatives. *J. Org. Chem.* **2016**, *81*, 6266−6272.
(38) Urbano, A.; Hernández-Torres, G.; del Hoyo, A. M.; Martínez-Carrión, A.; Carreño, M. C. Mild Access to Planar-Chiral *ortho*-Condensed Aromatic Ferrocenes *via* Gold(I)-Catalyzed Cycloisomerization of *ortho*-Alkynylaryl Ferrocenes. *Chem. Commun.* **2016**, *52*, 6419−6422.
(39) Zhang, P.-C.; Li, Y.-L.; He, J.; Wu, H.-H.; Li, Z.; Zhang, J. Simultaneous Construction of Axial and Planar Chirality by Gold/TY-Phos-Catalyzed Asymmetric Hydroarylation. *Nat. Commun.* **2021**, *12*, 4609.
(40) Huang, F.-R.; Zhang, P.; Yao, Q.-J.; Shi, B.-F. Construction of Planar Chiral Ferrocenes by Cobalt-Catalyzed Enantioselective C-H Acyloxylation Enabled by Dual Ligands. *CCS Chem.* **2024**, *6*, 2783−2793.
(41) Chen, H.; Wang, Y.-X.; Luan, Y.-X.; Ye, M. Enantioselective Twofold C-H Annulation of Formamides and Alkynes without Built-in Chelating Groups. *Angew. Chem., Int. Ed.* **2020**, *59*, 9428−9432.
(42) Kuang, X.; Li, J.-J.; Liu, T.; Ding, C.-H.; Wu, K.; Wang, P.; Yu, J.-Q. Cu-Mediated Enantioselective C-H Alkynylation of Ferrocenes with Chiral BINOL Ligands. *Nat. Commun.* **2023**, *14*, 7698.
(43) Zhang, Z.-Z.; Zhou, G.; Yue, Q.; Yao, Q.-J.; Shi, B.-F. Copper/BINOL-Catalyzed Enantioselective C-H Functionalization toward Planar Chiral Ferrocenes Under Mild Conditions. *ACS Catal.* **2024**, *14*, 4030−4039.
(44) Lou, S.-J.; Zhuo, Q.; Nishiura, M.; Luo, G.; Hou, Z. Enantioselective C-H Alkenylation of Ferrocenes with Alkynes by Half-Sandwich Scandium Catalyst. *J. Am. Chem. Soc.* **2021**, *143*, 2470−2476.
(45) Gao, D.-W.; Gu, Q.; Zheng, C.; You, S.-L. Synthesis of Planar Chiral Ferrocenes by Transition-Metal-Catalyzed Enantioselective C-H Activation. *Acc. Chem. Res.* **2017**, *50*, 351−365.
(46) Liu, C.-X.; Gu, Q.; You, S.-L. Asymmetric C-H Bond Functionalization of Ferrocenes: New Opportunities and Challenges. *Trends Chem.* **2020**, *2*, 737−749.
(47) Zhang, Z.-Z.; Huang, D.-Y.; Shi, B.-F. Recent Advances in the Synthesis of Ferrocene Derivatives *via* 3d Transition Metal-Catalyzed C-H Functionalization. *Org. Biomol. Chem.* **2022**, *20*, 4061−4073.
(48) Keith, J. M.; Larrow, J. F.; Jacobsen, E. N. Practical Considerations in Kinetic Resolution Reactions. *Adv. Synth. Catal.* **2001**, *343*, 5−26.
(49) Chu, Y.; Han, Z.; Ding, K. Progresses in the Application of Kinetic Resolution in Transition Metal Catalyzed Asymmetric (Transfer) Hydrogenation. *Chin. J. Org. Chem.* **2023**, *43*, 1934−1951.
(50) Saito, K.; Shibata, Y.; Yamanaka, M.; Akiyama, T. Chiral Phosphoric Acid-Catalyzed Oxidative Kinetic Resolution of Indolines Based on Transfer Hydrogenation to Imines. *J. Am. Chem. Soc.* **2013**, *135*, 11740−11743.
(51) Saito, K.; Miyashita, H.; Ito, Y.; Yamanaka, M.; Akiyama, T. Oxidative Kinetic Resolution of Acyclic Amines Based on Equilibrium Control. *Org. Lett.* **2020**, *22*, 3128−3134.
(52) Cheng, D.-J.; Yan, L.; Tian, S.-K.; Wu, M.-Y.; Wang, L.-X.; Fan, Z.-L.; Zheng, S.-C; Liu, X.-Y.; Tan, B. Highly Enantioselective Kinetic Resolution of Axially Chiral BINAM Derivatives Catalyzed by a Brønsted Acid. *Angew. Chem., Int. Ed.* **2014**, *53*, 3684−3687.
(53) Zhao, Y.; Ding, Y.-X.; Wu, B.; Zhou, Y.-G. Nickel-Catalyzed Asymmetric Hydrogenation for Kinetic Resolution of [2.2]-Paracyclophane-Derived Cyclic *N*-Sulfonylimines. *J. Org. Chem.* **2021**, *86*, 10788−10798.
(54) Li, J.; Zhao, C. Highly Enantioselective Synthesis of Planar-Chiral Cyclophanes through a Brønsted Acid-Catalyzed Asymmetric Transfer Hydrogenation. *ACS Catal.* **2023**, *13*, 14155−14162.
(55) Liu, W.-M.; Hao, Y.-J.; Zhang, Y.; Li, X.-G.; Ji, S.-J.; Cai, Z.-J. Asymmetric Synthesis of Azahelicenes *via* CPA-Catalyzed Kinetic Resolution. *Org. Lett.* **2025**, *27*, 363−368.
(56) Yamazaki, Y.; Uebayasi, M.; Hosono, K. Enantiotopic Differentiation in Horse-Liver Alcohol-Dehydrogenase-Catalyzed Oxidoreduction Studied with Novel Substrates Having Organometallic Moieties. *Eur. J. Biochem.* **1989**, *184*, 671−680.

https://doi.org/10.1021/jacsau.5c00698
JACS Au 2025, 5, 3765−3774

(57) Skrobo, B.; Rolfes, J. D.; Deska, J. Enzymatic Approaches for the Preparation of Optically Active Non-centrochiral Compounds. *Tetrahedron* **2016**, *72*, 1257−1275.
(58) Akiyama, M.; Akagawa, K.; Seino, H.; Kudo, K. Peptide-Catalyzed Kinetic Resolution of Planar-Chiral Metallocenes. *Chem. Commun.* **2014**, *50*, 7893−7896.
(59) Bueno, A.; Rosol, M.; García, J.; Moyano, A. Asymmetric Dihydroxylation of 2-Substituted 1-Vinylferrocenes: the First Non-Enzymatic Kinetic Resolution of Planar-Chiral Ferrocenes. *Adv. Synth. Catal.* **2006**, *348*, 2590−2596.
(60) Ogasawara, M.; Watanabe, S.; Fan, L.; Nakajima, K.; Takahashi, T. Kinetic Resolution of Planar-Chiral Ferrocenes by Molybdenum-Catalyzed Enantioselective Metathesis. *Organometallics* **2006**, *25*, 5201−5203.
(61) Ogasawara, M. Enantioselective Preparation of Planar-Chiral Transition Metal Complexes by Asymmetric Olefin-Metathesis Reactions in Metal Coordination Spheres. *Chem. Rec.* **2021**, *21*, 3509−3519.
(62) Alba, A.-N.; Gómez-Sal, P.; Rios, R.; Moyano, R. Organocatalytic Kinetic Resolution of a Planar-Chiral Ferrocenecarbaldehyde. *Tetrahedron: Asymmetry* **2009**, *20*, 1314−1318.
(63) Patti, A.; Pedotti, S. Parallel or Classical Kinetic Resolution of a Planar Chiral Ferrocenylketone through Asymmetric Reductions. *Tetrahedron: Asymmetry* **2010**, *21*, 2631−2637.
(64) Liu, R.; Zhou, G.; Hall, T. H.; Clarkson, G.; Wills, M.; Chen, W. Practical Access to Planar Chiral 1,2-(α-Ketotetramethylene)-ferrocene by Non-Enzymatic Kinetic Resolution and Conclusive Confirmation of its Absolute Configuration. *Adv. Synth. Catal.* **2015**, *357*, 3453−3457.
(65) Liu, C.-X.; Zhao, F.; Feng, Z.; Wang, Q.; Gu, Q.; You, S.-L. Kinetic Resolution of Planar Chiral Metallocenes using Rh-Catalysed Enantioselective C-H Arylation. *Nat. Synth.* **2023**, *2*, 49−57.
(66) Yao, Q.-J.; Huang, F.-R.; Chen, J.-H.; Shi, B.-F. Nickel(II)/BINOL-Catalyzed Enantioselective C-H Activation *via* Desymmetrization and Kinetic Resolution. *Nat. Commun.* **2024**, *15*, 7135.
(67) Lv, Y.; Mou, C.; Liu, Q.; Shu, L.; Cai, Y.; Lv, X.; Jin, Z.; Chi, Y. R. Asymmetric Synthesis of Planar Chiral Carbonitriles and Amines *via* Carbene-Catalyzed Kinetic Resolution. *Org. Lett.* **2024**, *26*, 1584−1588.
(68) Rueping, M.; Dufour, J.; Schoepke, F. R. Advances in Catalytic Metal-Free Reductions: from Bio-Inspired Concepts to Applications in the Organocatalytic Synthesis of Pharmaceuticals and Natural Products. *Green Chem.* **2011**, *13*, 1084−1105.
(69) Rueping, M.; Antonchick, A. P.; Theissmann, T. A Highly Enantioselective Brønsted Acid Catalyzed Cascade Reaction: Organocatalytic Transfer Hydrogenation of Quinolines and their Application in the Synthesis of Alkaloids. *Angew. Chem., Int. Ed.* **2006**, *45*, 3683−3686.
(70) Zheng, C.; You, S.-L. Transfer Hydrogenation with Hantzsch Esters and Related Organic Hydride Donors. *Chem. Soc. Rev.* **2012**, *41*, 2498−2518.
(71) Wang, D.-S.; Chen, Q.-A.; Lu, S.-M.; Zhou, Y.-G. Asymmetric Hydrogenation of Heteroarenes and Arenes. *Chem. Rev.* **2012**, *112*, 2557−2590.
(72) Chen, Q.-A.; Ye, Z.-S.; Duan, Y.; Zhou, Y.-G. Homogeneous Palladium-Catalyzed Asymmetric Hydrogenation. *Chem. Soc. Rev.* **2013**, *42*, 497−511.
(73) Wang, J.; Chen, M.-W.; Ji, Y.; Hu, S.-B.; Zhou, Y.-G. Kinetic Resolution of Axially Chiral 5- or 8-Substituted Quinolines *via* Asymmetric Transfer Hydrogenation. *J. Am. Chem. Soc.* **2016**, *138*, 10413−10416.
(74) Bernardo, O.; González-Pelayo, S.; López, L. A. Synthesis and Applications of Ferrocene-Fused Nitrogen Heterocycles. *Eur. J. Inorg. Chem.* **2022**, *2022*, No. e202100911.
(75) Wang, J.; Zhu, Z.-H.; Chen, M.-W.; Chen, Q.-A.; Zhou, Y.-G. Catalytic Biomimetic Asymmetric Reduction of Alkenes and Imines Enabled by Chiral and Regenerable NAD(P)H Models. *Angew. Chem., Int. Ed.* **2019**, *58*, 1813−1817.
(76) Zhao, Z.-B.; Li, X.; Chen, M.-W.; Zhao, Z. K.; Zhou, Y.-G. Biomimetic Asymmetric Reduction of Benzoxazinones and Quinoxalinones using Ureas as Transfer Catalysts. *Chem. Commun.* **2020**, *56*, 7309−7312.
(77) Zhao, Z.-B.; Li, X.; Wu, B.; Zhou, Y.-G. Biomimetic Asymmetric Reduction of Quinazolinones with Chiral and Regenerable NAD(P)H Models. *Chin. J. Chem.* **2020**, *38*, 714−718.
(78) Wang, J.; Zhao, Z.-B.; Zhao, Y.; Luo, G.; Zhu, Z.-H.; Luo, Y.; Zhou, Y.-G. Chiral and Regenerable NAD(P)H Models Enabled Biomimetic Asymmetric Reduction: Design, Synthesis, Scope, and Mechanistic Studies. *J. Org. Chem.* **2020**, *85*, 2355−2368.
(79) Chen, M.-W.; Wu, B.; Liu, Z.; Zhou, Y.-G. Biomimetic Asymmetric Reduction Based on the Regenerable Coenzyme NAD(P)H Models. *Acc. Chem. Res.* **2023**, *56*, 2096−2109.
(80) Li, N.; Hong, B.; Zhao, J.; Gu, Z. Nitrenoid from Oxime: A Practical Synthesis of Planar Chiral Ferrocenyl Phenanthridines *via* Nitrene-Involved Ring-Expansion Reaction. *Angew. Chem., Int. Ed.* **2023**, *62*, No. e202215530.
(81) Marcelli, T.; Hammar, P.; Himo, F. Phosphoric Acid-Catalyzed Enantioselective Transfer Hydrogenation of Imines: a Density Functional Theory Study of the Reaction Mechanism and Origins of Stereoselectivity. *Chem. Eur. J.* **2008**, *14*, 8562−8571.

https://doi.org/10.1021/jacsau.5c00698
JACS Au 2025, 5, 3765−3774